Article

Well-Designed Phosphine–Urea Ligand for Highly Diastereo- and Enantioselective 1,3-Dipolar Cycloaddition of Methacrylonitrile: A Combined Experimental and Theoretical Study

Yang Xiong, Zhuanzhuan Du, Haohua Chen, Zhao Yang, Qiuyuan Tan, Changhui Zhang, Lei Zhu, Yu Lan, and Min Zhang

J. Am. Chem. Soc., **Just Accepted Manuscript** • DOI: 10.1021/jacs.8b10939 • Publication Date (Web): 13 Dec 2018

Well-Designed Phosphine–Urea Ligand for Highly Diastereo- and Enantioselective 1,3-Dipolar Cycloaddition of Methacrylonitrile: A Combined Experimental and Theoretical Study

Yang Xiong,[†,§] Zhuanzhuan Du,[†,§] Haohua Chen,[‡,§] Zhao Yang,[†] Qiuyuan Tan,[†] Changhui Zhang,[†] Lei Zhu,[‡] Yu Lan,*[‡,#] and Min Zhang*[†]

[†]Chongqing Key Laboratory of Natural Product Synthesis and Drug Research, School of Pharmaceutical Sciences, and [‡]School of Chemistry and Chemical Engineering, Chongqing University, Chongqing 401331, China

[#]College of Chemistry and Molecular Engineering, Zhengzhou University, Zhengzhou 450001, China

ABSTRACT: A novel chiral phosphine–urea bifunctional ligand has been developed for Cu-catalyzed asymmetric 1,3-dipolar cycloaddition of iminoesters with methacrylonitrile, a long-standing challenging substrate in asymmetric catalysis. Distortion–interaction energy analysis based on density functional theory (DFT) calculations reveals that the distortion energy plays an important role in the observed enantioselectivity, which can be attributed to the steric effect between the phosphine ligand and the dipole reactant. DFT calculations also indicate that nucleophilic addition is the enantioselectivity-determining step and hydrogen bonding between the urea moiety and methacrylonitrile assists in control of the diastereo- and enantioselectivity. By a combination of metal–catalysis and organocatalysis, excellent diastereo- and enantioselectivities (up to 99:1 diastereomeric ratio, 99% enantiomeric excess) as well as good yields are achieved. A wide range of substitution patterns of both iminoester and acrylonitrile are tolerated by this catalyst system, providing access to a series of highly substituted chiral cyanopyrrolidines with up to two quaternary stereogenic centers. The synthetic utility is demonstrated by enantioselective synthesis of antitumor agent **ETP69** with a pivotal nitrile pharmacophore and an all-carbon quaternary stereogenic center.

■ INTRODUCTION

Despite the great advances in asymmetric synthesis over the last few decades, stereochemical control of substrates that lack an effective catalyst–substrate interaction or strong steric/electronic biases remains a challenge.[1] Methacrylonitrile **1a** falls into this category, presumably because of the inferior catalyst–substrate spatial orientation arising from the linearity of the nitrile group and the low level of enantiofacial differentiation because of the steric similarity between the methyl and nitrile substituents. The poor intrinsic reactivity and challenges associated with formation of an all-carbon quaternary stereogenic center to form a C–C bond at the α position of methacrylonitrile further restrict its synthetic utility (Scheme 1a). Consequently, attempts to develop catalytic stereoselective reactions using methacrylonitrile have resulted in limited success.[2]

Catalytic diastereo- and enantioselective 1,3-dipolar cycloadditions of iminoesters have been intensively investigated in recent years, with many electron-deficient alkenes used as capable dipolarophiles.[4−8] However, for cycloadditions with methacrylonitrile, which can also provide an electron-deficient C=C bond, the diastereoselectivity rather than the enantioselectivity remains a challenge. In 2015, Overman, Houk, and co-workers[9a] realized the first highly diastereoselective 1,3-dipolar cycloaddition with methacrylonitrile using achiral phosphine ligand-complexed Cu^{I} to activate the iminoester (Scheme 1b). Theoretical calculations showed that the presence of an electrostatic interaction between the phosphine ligand and the reacting methacrylonitrile in the transition state leads to high diastereoselectivity, otherwise the diastereoselectivity is low. Using the racemic cycloadduct **3**, Overman, Horne, and co-workers[9b] developed an elegant synthesis of natural product analogue **ETP69**, a very

Scheme 1. 1,3-Dipolar Cycloaddition of Iminoesters with Acrylonitriles

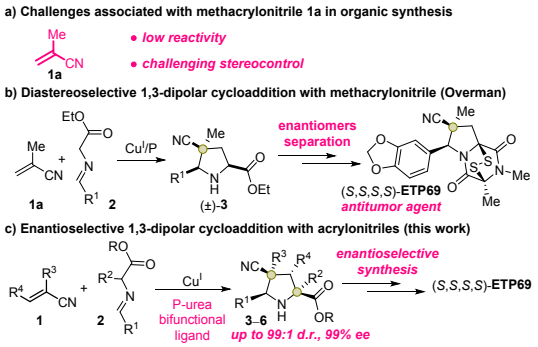

promising clinical candidate for cancer chemotherapy. The authors also showed that the preeminent cytotoxicity of this compound depends on the nitrile pharmacophore and largely resides in the (*S,S,S,S*)-enantiomer, which is obtained by separation of the enantiomers.[9b] Despite this methodology advancement and the synthetic value of chiral cyanopyrrolidines,[9] highly diastereo- and enantioselective 1,3-dipolar cycloadditions with methacrylonitrile have not been reported.

Most of the previous strategies for catalytic stereoselective 1,3-dipolar cycloadditions of iminoesters use a single model for organocatalysis or metal catalysis by acting on one of the reaction partners (dipole or dipolarophile).[3–9] From our previous research of dipolar cycloadditions,[10] we speculate that a bifunctional catalysis,[11,12] which integrates the unique activation modes of organocatalysis with the well-established chemistry of metal catalysis, could activate both the dipole and dipolarophile and thus address the aforementioned challenges associated with methacrylonitrile. With this idea in mind, we designed a novel type of bifunctional ligands based on privileged chiral 1,2-ethylenediamine scaffolds (Figure 1a).[13] Theoretical studies have previously been performed to validate the feasibility. The preliminary computational results revealed that both the phosphine moiety and benzoyl group of the phosphinoamide unit could coordinate with copper to activate iminoesters,[14] while the two NH groups in the (thio)urea unit could form hydrogen bonds with the nitrile group of the acrylonitriles (Figure 1b).[15] Through synergistic activation and spatial orientation of the dipole and dipolarophile, high diastereo- and enantioselectivity could be achieved for 1,3-dipolar cycloaddition of iminoesters with acrylonitriles particularly methacrylonitrile. If this strategy could be successfully implemented, a series of chiral cyanopyrrolidines with up to two quaternary stereogenic centers could be generated (Scheme 1c). This would be a significant advance in the field of quaternary stereogenic center generation, because catalytic enantioselective methods to generate quaternary stereocenters by incorporating reaction partners in an intermolecular manner are currently very limited.[16]

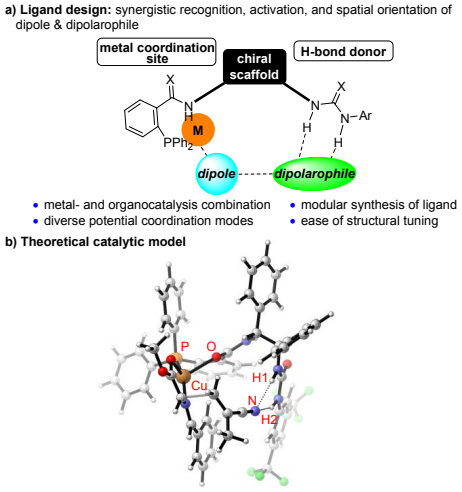

Figure 1. a) Ligand design; b) theoretical catalytic model.

■ RESULTS AND DISCUSSION

Reaction Optimization. We first evaluated ligand **L1**, which was prepared by coupling three inexpensive components: (*R,R*)-1,2-diaminocyclohexane, 2-diphenylphosphino-benzoic acid, and 3,5-bis(trifluromethyl)-phenyl isocyanate. For the catalytic system of **L1**/$Cu(CH_3CN)_4BF_4$, 1,3-dipolar cycloaddition of **1a** and **2a** occurred with promising enantioselectivity (76% *ee*), albeit in low yield (Table 1, entry 1). Taking into account the fact that both squaramide and thiourea are widely used as effective hydrogen donors,[15] and

Table 1. Optimization of 1,3-Dipolar Cycloaddition of Methacrylonitrile[a]

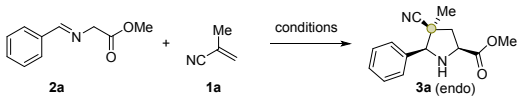

entry	ligand	metal	yield (%)[b]	d.r.[c]	*ee* (%)[d]
1	**L1**	$Cu(MeCN)_4BF_4$	10	—	76
2	**L2–L5**	$Cu(MeCN)_4BF_4$	<5	—	—
3	**L6**	$Cu(MeCN)_4BF_4$	45	98:2	98
4	**L6**	$Cu(MeCN)_4PF_6$	18	98:2	98
5	**L6**	$Cu(MeCN)_4ClO_4$	16	98:2	98
6	**L6**	AgF	46	98:2	88
7[e]	**L6**	$Cu(MeCN)_4BF_4$	95	98:2	99
8[e]	*ent*-**L6**	$Cu(MeCN)_4BF_4$	94	98:2	-99
9[e]	none	$Cu(MeCN)_4BF_4$	<5	—	—
10[e]	**L7–L9**	$Cu(MeCN)_4BF_4$	<5	—	—
11[e]	**L10**	$Cu(MeCN)_4BF_4$	35	10:90	97
12[e]	**L11**	$Cu(MeCN)_4BF_4$	30	40:60	87
13[e]	**L12**	$Cu(MeCN)_4BF_4$	25	60:40	20
14[e]	**L13**	$Cu(MeCN)_4BF_4$	32	45:55	88

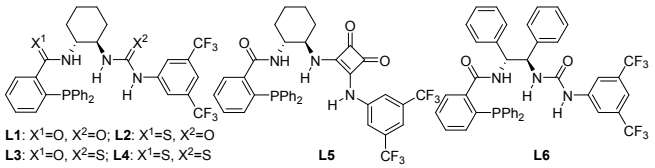

[a]Conditions unless otherwise stated: **1a** (0.4 mmol), **2a** (0.2 mmol), ligand (5.5 mol%), metal (5 mol%), Et_3N (50 mol%), 4 Å MS (200 mg), THF (4 mL), room temperature, 72 h. [b]Isolated yield of the major isomer. [c]Ratio of endo/exo isomers, determined by HPLC analysis of the crude reaction mixture. [d]Determined by chiral HPLC analysis of the major isomer. [e]Using K_2CO_3 as the base and ^{t}BuOMe as the solvent.

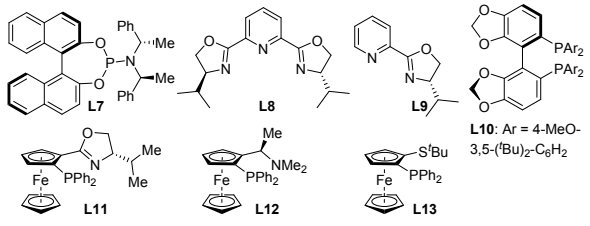

Figure 2. Known chiral ligands screened in 1,3-dipolar cycloaddition of methacrylonitrile.

considering that incorporation of a sulfur atom into the ligand could provide more diverse metal coordination

modes,[17] we synthesized ligands **L2–L4** with one or two sulfur atoms incorporated and ligand **L5** with a squaramide group to take advantage of the previous observations. However, none of these ligands gave the desired cycloaddition product in acceptable yield (entry 2). Upon switching the chiral scaffold to diphenylethylenediamine, ligand **L6** resulted in significantly improved yield and degree of stereoselectivity (entry 3). Copper salts with different counter anions gave lower yield of **3a** (entries 4 and 5), while silver salt AgF

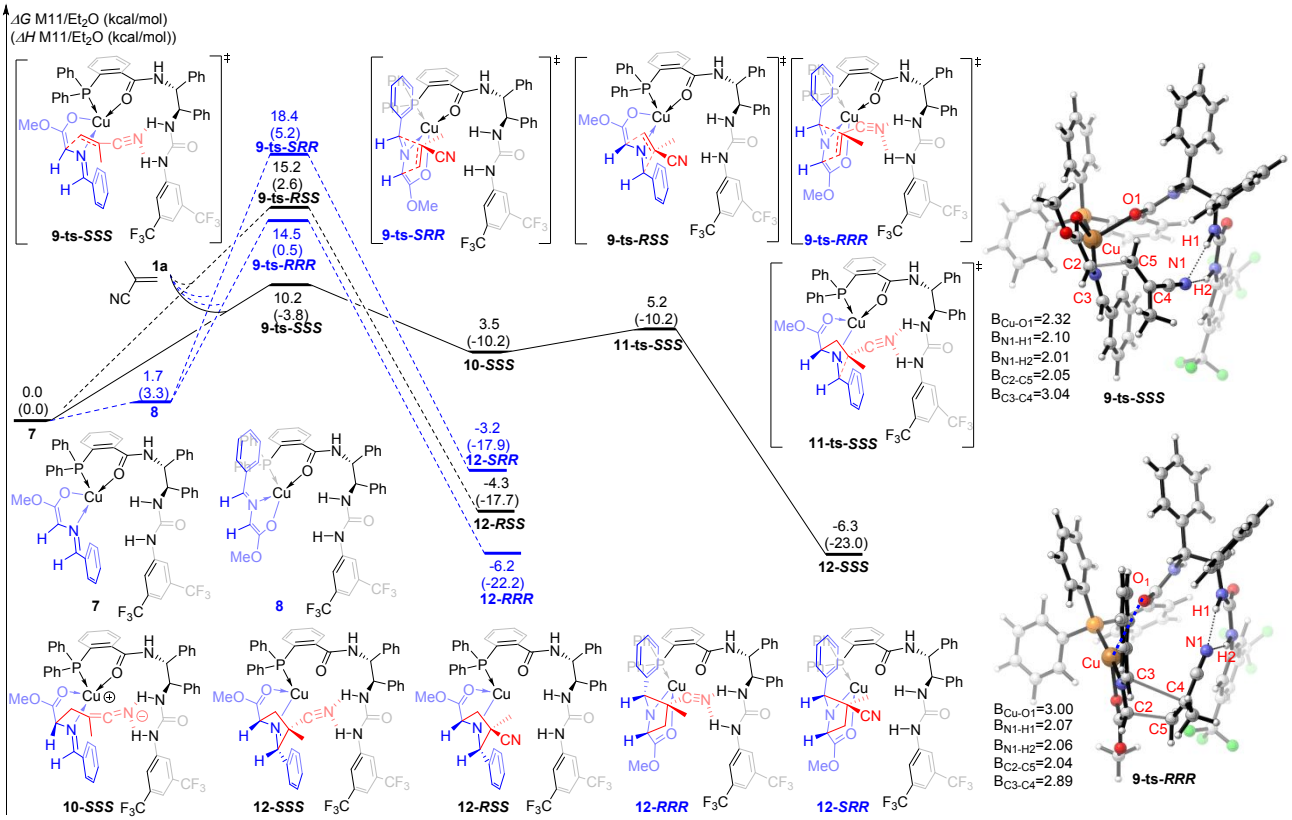

Figure 3. Free energy profiles for catalytic asymmetric 1,3-dipolar cycloaddition of methacrylonitrile. The energy values are given in kcal/mol and represent the relative free energies calculated by the DFT/M11 method in Et_2O. The bond lengths are given in angstroms.

produced comparable yield and d.r. with slightly lower enantioselectivity (entry 6). Considering copper is a more abundant metal compared to silver, $Cu(CH_3CN)_4BF_4$ was used as the metal precatalyst for further reaction optimization, which led us to identify the optimal conditions ($Cu(CH_3CN)_4BF_4$/**L6**/K_2CO_3/^{t}BuOMe/rt), giving **3a** in 95% yield with excellent stereoselectivities (entry 7, 98:2 d.r., 99% *ee*). Performing 1,3-dipolar cycloaddition with a series of privileged chiral ligands (Figure 2, **L7–L13**) under the optimal conditions or the typical conditions found in the literatures gave either low yields (0–35%) or poor stereoselectivities (entries 10–14), [18] further highlighting the uniqueness of this novel type of bifunctional ligand.

Mechanistic Study. All the density functional thery (DFT) calculations were performed with Gaussian 09 series of programs.[19] The B3-LYP[20] functional with the standard 6–31G(d) basis set (SDD[21] basis set for Cu atoms) was used for the geometry optimizations. Harmonic vibrational frequency calculations were performed for all of the stationary points to confirm whether they are a local minima or transition structures, and to derive the thermochemical corrections for the enthalpies and free energies. The M11[22] functional with the 6–311+G(d,p) basis set (SDD basis set for Cu atoms) was used to calculate the solvation single-point and give more accurate energy information. The solvent effects were considered by single-point calculations of the gas-phase stationary points with the SMD[23] solvation model in diethylether (Et_2O) solvent.

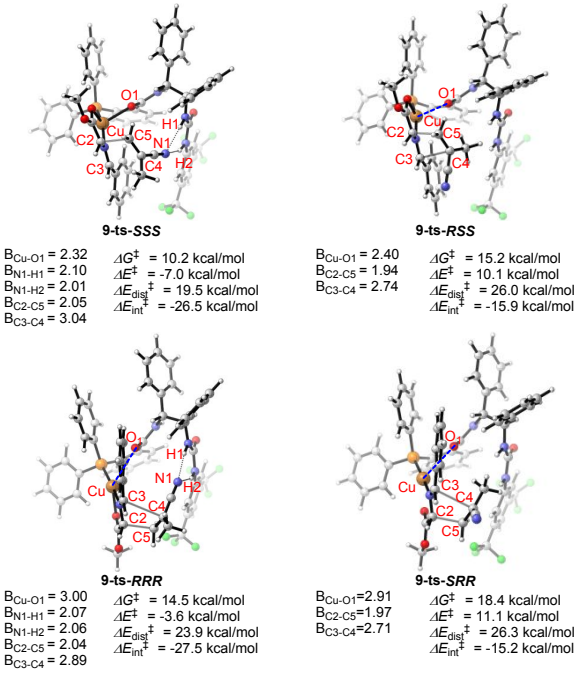

Figure 4. Distortion–interaction energy analysis of the optimized structures of transition state **9-ts-*SSS***, **9-ts-*RSS***, **9-ts-*RRR***, and **9-ts-*SRR*** in the nucleophilic addition step.

The free energy profiles for asymmetric 1,3-dipolar cycloaddition of azomethine ylides using the synthesized phosphine–urea bifunctional ligand **L6** are shown in Figure 3. The calculated results suggest that nucleophilic addition is the enantioselectivity-determining step. Coordination and deprotonation of the iminoester with the Cu^{I} catalyst gives complex **7** and its isomer **8**. The relative free energy of **8** is 1.7 kcal/mol higher than that of **7**, which can be attributed to strain repulsion between the amide group of the iminoester and the phenyl group of the phosphine ligand. Nucleophilic addition of the α-carbon atom of iminoester **2a** to the terminal carbon of **1a** via transition state **9-ts-*SSS*** gives intermediate **10-*SSS***. The calculated activation free energy of the first nucleophilic addition step is 10.2 kcal/mol. Subsequent cycloaddition rapidly generates the (***S***,***S***,***S***)-product-coordinated intermediate **12-*SSS*** via transition state **11-ts-*SSS*** with a free energy barrier of only 1.7 kcal/mol. The geometry information of **9-ts-*SSS*** shows that the distances between the nitrogen atom of the cyano group and the two hydrogen atoms of the urea moiety is 2.10 and 2.01 Å. These two hydrogen bonds significantly stabilize the negative charge in the formed intermediate, which leads to this process having a low activation free energy. In another possible case, 1,3-cycloaddition of methacrylonitrile **1a** and complex **7** via transition state **9-ts-*RSS*** gives (*R*,*S*,*S*)-product-coordinated intermediate **12-*RSS*** with an activation free energy of 15.2 kcal/mol. The relative free energy of **9-ts-*RSS*** is 5.0 kcal/mol higher than that of **9-ts-*SSS*** because of the absence of hydrogen bonding in **9-ts-*RSS***. The computational results reveal high stereoselectivity, which agrees with the experimental observations. Alternatively, the (*R*,*R*,*R*)-enantiomer could form by 1,3-cycloaddition of methacrylonitrile **1a** and intermediate **8** via concerted transition state **9-ts-*RRR***, which has been confirmed by an intrinsic reaction coordinate calculation. The relative free energy of **9-ts-*RRR*** is 4.3 kcal/mol higher than that of **9-ts-*SSS***, which suggests up to 99% *ee* with the major product in the (*S*,*S*,*S*)-configuration, although intermolecular hydrogen bonding also exists for **9-ts-*RRR***.

To obtain additional insight, distortion–interaction energy analysis was performed to explain the reactivity of the bimolecular system ($\Delta E_{act}^{\ddagger}=\Delta E_{int}^{\ddagger}+\Delta E_{dist}^{\ddagger}$) (Figure 4).[24] The computational results show that the difference in the interaction-energy terms ($\Delta E_{int}^{\ddagger}$) for **9-ts-*SSS*** and **9-ts-*RRR*** is only 1.0 kcal/mol. However, the difference in the distortion-energy terms ($\Delta E_{dist}^{\ddagger}$) for the two transition states is 4.4 kcal/mol. Comparing the geometries of **9-ts-*SSS*** and **9-ts-*RRR***, the oxygen atom of the amide moiety of the ligand is close to the Cu atom in **9-ts-*SSS*** (B_{Cu-O1}=2.32 Å), indicating significant coordination. However, the corresponding bond length is 3.00 Å in **9-ts-*RRR***, meaning that the distortion energy in this transition state is much higher. Thus, these results suggest that the distortion energy plays an important role in the observed enantioselectivity. In our theoretical calculations, we found that another diastereomer could be generated *via* transition state **9-ts-*RSS***. We also calculated the distortion and interaction energies for this transition state. The results show that the interaction energy in **9-ts-*RSS*** is much lower than that in **9-ts-*SSS*** because of the absence of hydrogen bonding between the urea moiety and methacrylonitrile, which lead to the higher relative energy of **9-ts-*RSS***.

Mechanism Verification. Based on the aforementioned theoretical results, we hypothesized that both metal catalysis and organocatalysis (hydrogen bonding) are crucial components in the cycloaddition. To confirm our hypothesis, a few *N*-methylated phosphine–urea ligands were designed and calculations were performed for 1,3-dipolar cycloaddition. As shown in Figure 5, **L14** and **L15** have only one of the two nitrogen atoms containing a methyl group, while **L16** has both nitrogen atoms of the urea moiety masked by methyl groups. The corresponding free energy profiles are shown in Figure 6. The differences in the free energy of activation values for the two enantiomeric transition states of **L14** and **L15** are 5.2 and 6.1 kcal/mol, respectively (Figures 6a and 6b). These free energy differences suggest that up to 99% *ee* could be experimentally obtained in any cycloaddition product. The calculated difference of the free energy of activation values for **9-ts-*RRR*-L16** and **9-ts-*SSS*-L16** is only 0.6 kcal/mol, which suggests that poor enantioselectivity would be experimentally observed, largely because of the absence of hydrogen bonding in **9-ts-*RRR*-L16** and **9-ts-*SSS*-L16** (Figure 6c).

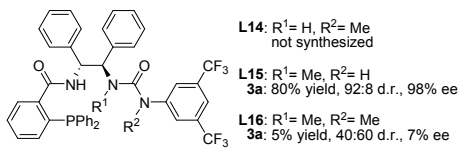

Figure 5. Structures of the *N*-methylated ligands and 1,3-dipolar cycloaddition of **1a** and **2a** using **L15** and **L16** under the optimal conditions.

Distortion-interaction energy analysis was also performed to explain the origin of the enantioselectivity for asymmetric 1,3-dipolar cycloaddition using the designed phosphine–urea ligands **L14**, **L15**, and **L16** (Figure 7). When the *N*-methyl-monosubstituted ligands **L14** and **L15** with a single hydrogen bond interaction are used, the interaction-energy terms ($\Delta E_{int}^{\ddagger}$) in the four transition states (**9-ts-*RRR*-L14**, **9-ts-*SSS*-L14**, **9-ts-*RRR*-L15** and **9-ts-*SSS*-L15**) are relatively low. However, the corresponding distortion energy terms ($\Delta E_{dist}^{\ddagger}$) are slightly enhanced owing to weaker activation of the methacrylonitrile reactant compared with the **L6** case. Analogously, the calculated results suggest that the distortion energy mainly controls the reactivity because of the same trend of the activation free energy. Thus the large discrepancy in the distortion energy results in high predicted *ee* when **L14** and **L15** are used. Furthermore, when both of the nitrogen atoms of the urea moiety are masked by methyl groups in **L16**, the activation free energies of **9-ts-*RRR*-L16** and **9-ts-*SSS*-L16** in the cycloaddition step are significantly enhanced, which can be attributed to two reasons. First, the interaction-energy term ($\Delta E_{int}^{\ddagger}$) is significantly lower in the absence of hydrogen bonding. Second, acrylonitrile further distorts to react with the dipole owing to the omitted hydrogen bond activation, which leads to increase in the distortion energy term ($\Delta E_{dist}^{\ddagger}$) in the late-coming transition state. Therefore, the reaction center is far from the chiral center of the ligand owing to the lack of hydrogen bonding, which results in the poorly regulatory effect of the ligand and thus the low *ee* of the product. Based on the aforementioned hypothesis, *N*-methyl-substituted phosphine–urea ligands of **L15** and **L16** were synthesized and used in 1,3-dipolar cycloaddition of **1a** and **2a** under the optimal conditions ($Cu(CH_3CN)_4BF_4$/**L6**/K_2CO_3/^{t}BuOMe/rt). *Ee* values of 98% and 7% are obtained for **L15** and **L16**, respectively (Figure 5),

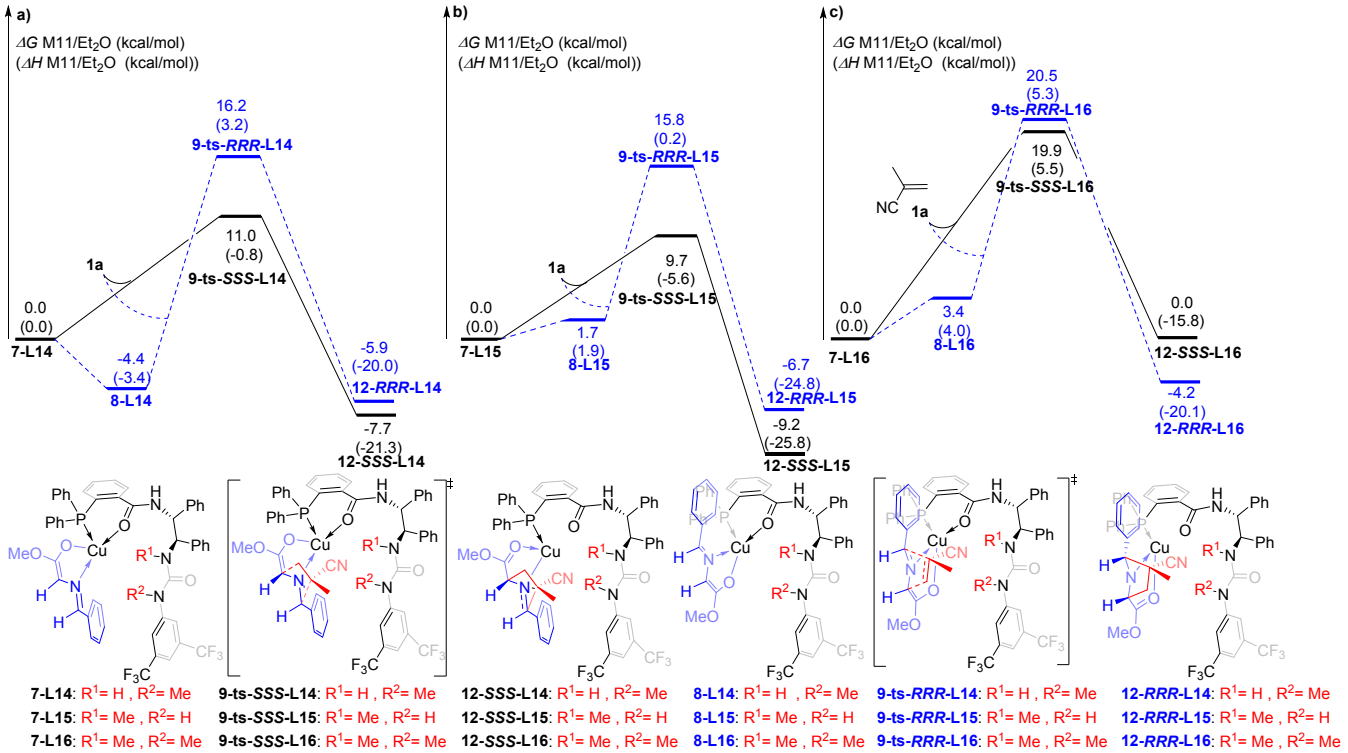

Figure 6. Free energy profiles for catalytic asymmetric 1,3-dipolar cycloaddition of methacrylonitrile using *N*-methylated ligands

a) **L14**, b) **L15**, and c) **L16**. The values are in kcal/mol and represent the relative free energies calculated by the DFT/M11 method in Et_2O.

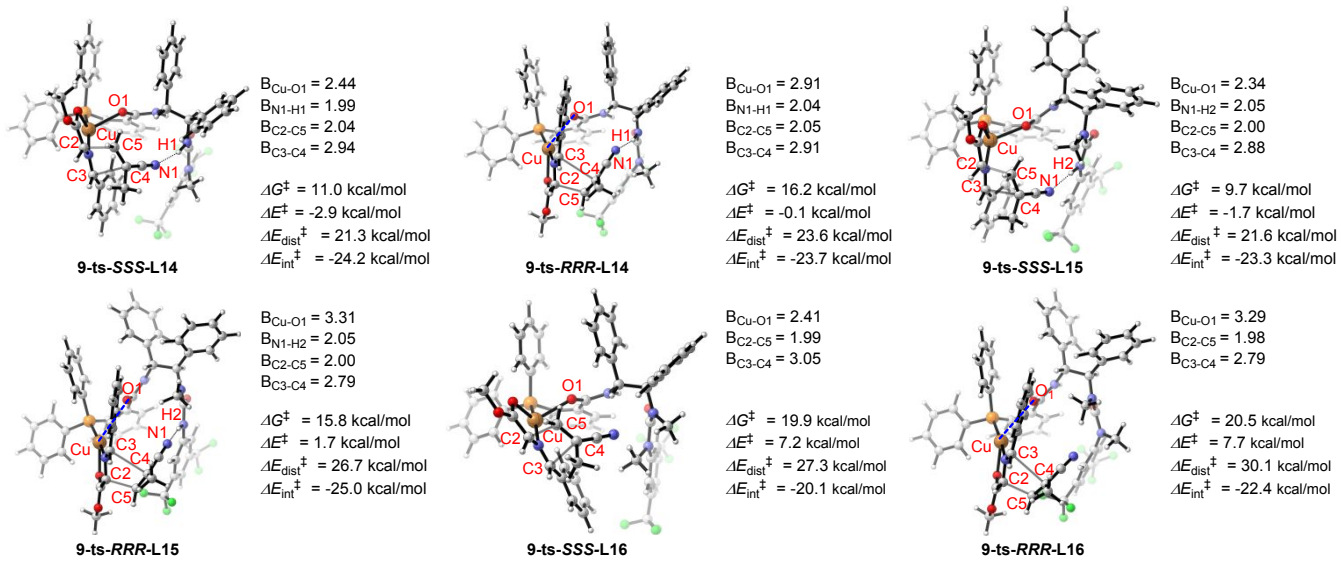

Figure 7. Distortion–interaction energy analysis of the optimized structures in the nucleophilic addition step using *N*-methylated phosphine–urea ligands **L14**, **L15**, and **L16**.

which is in agreement with the computational predictions. Notably, for **L16**, the yield significantly decreases to 5%, which can be explained by the higher activation free energy for the cycloaddition step with ligand **L16**. From high-resolution mass spectrometry (HRMS) analysis, the azomethine ylide–Cu–**L6** complex (m/z=995.2246) is present in the crude reaction mixture, suggesting that iminoester could be preactivated by the coordination with **L6**–Cu complex.[18] Therefore, the combination of experimental observations and theoretical calculations shows that both the reactivity and stereoselectivity arise from the synergistic activation and spatial orientation of the dipole and dipolarophile by the amidophosphine–urea bifunctional ligand **L6**–Cu complex.

Substrate Scope. Having established the optimal catalytic system and elucidated the reaction mechanism, we next explored the scope of iminoester **2** in 1,3-dipolar cycloaddition with methacrylonitrile (Table 2). Iminoesters possessing both electron-deficient and electron-rich groups on the phenyl ring gave the cycloaddition products in good to excellent yields and with excellent stereoselectivities (96:4–98:2 d.r., 97–99% *ee*) (entries 1–7). The substitution pattern of the

Table 2. Catalytic Asymmetric 1,3-Dipolar Cycloaddition of Various Iminoesters with Methacrylonitrile[a]

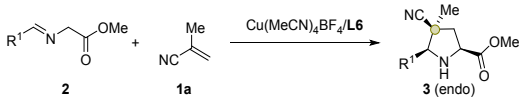

entry	**3**	R^1	yield (%)[b]	d.r.[c]	*ee* (%)[d]
1	**3a**	Ph	95	98:2	99
2	**3b**	4-FC_6H_4	95	98:2	99
3	**3c**	4-ClC_6H_4	86	97:3	97
4	**3d**	4-BrC_6H_4	85	97:3	98
5	**3e**	4-$MeOC_6H_4$	91	98:2	97
6	**3f**	4-$COOMeC_6H_4$	86	96:4	98
7	**3g**	4-$CF_3C_6H_4$	75	96:4	98

8	**3h**	2-BrC_6H_4	83	99:1	99
9	**3i**	3-BrC_6H_4	76	99:1	99
10	**3j**	1-naphthyl	90	99:1	97
11	**3k**	2-naphthyl	95	98:2	99
12	**3l**	*N*-Bn-2-pyrryl	51	97:3	98
13	**3m**	2-thienyl	92	98:2	99
14	**3n**	2-furyl	51	99:1	99
15	**3o**	*N*-Bs-2-indolyl	75	98:2	97

[a]Conditions: **1a** (0.4 mmol), **2** (0.2 mmol), **L6** (5.5 mol%), $Cu(MeCN)_4BF_4$ (5 mol%), K_2CO_3 (50 mol%), 4 Å MS (200 mg), [t]BuOMe (4 mL), room temperature, 16–48 h. [b]Isolated yield. [c]Determined by HPLC analysis of the crude reaction mixture. [d]Determined by chiral HPLC analysis of the endo isomer. Bs=benzenesulfonyl.

phenyl ring has a negligible effect on the reactivity and stereoselectivity, and bromo groups at *ortho*- *meta*-, and *para*-positions of the phenyl ring are all tolerated in this cycloaddition (entries 4, 8, and 9), thus providing handles on the phenyl ring for further elaboration of the cycloaddition products. Fused aromatic substrates, including 1- and 2-naphthyl-substituted iminoesters also proved to be viable azomethine ylide precursors (entries 10 and 11). Notably, iminoesters substituted with an array of heteroaryl groups, including pyrryl, thienyl, furyl, and indolyl groups, all worked well (entries 12–15). However, alkyl iminoesters do not work well under the current reaction conditions as a contrast of aryl iminoesters.

Chloro-bearing stereogenic carbon centers are found in a large number of natural products and bioactive compounds.[25] Although recent years have witnessed great advances in the development of catalytic enantioselective addition of carbon-halogen bonds to organic molecules, enantioselective construction of halogen-bearing quaternary stereogenic centers remains a challenge in organic synthesis.[26] As our interest in construction of quaternary stereogenic centers,[27] we tested whether commercially available *α*-chloroacrylnitrile is a suitable dipolarophile for 1,3-dipolar cycloaddition of iminoesters (Table 3). *α*-Chloroacrylnitrile reacted smoothly with iminoester **2a** under slightly modified conditions to give the corresponding product **4a** in high yield (89%) with excellent diastereo- and enantioselectivity (>96:4 d.r., 96% *ee*). We then briefly explored the iminoester scope. We found that iminoesters substituted with aryl (*p*-Br-phenyl and naphthyl) and heteroaryl (furyl, thienyl, and indolyl) groups all reacted smoothly with *α*-chloroacrylnitrile, giving a series of pyrrolidines with a chloro-bearing quaternary stereogenic center in good yields with excellent diastereo- and enantioselectivities (**4b**–**4g**). It is noteworthy that this study represents the first example of catalytic enantioselective 1,3-dipolar cycloaddition of iminoesters with *α*-chloroacrylnitrile. To further expand the substrate scope of the substituted acrylonitriles, *α*-phenyl- and *β*-ethyl-acrylonitriles were subjected to the optimal conditions. In these two cases, good yields and stereoselectivities were achieved (**4h** and **4i**).

Table 3. Catalytic Asymmetric 1,3-Dipolar Cycloaddition of Various Iminoesters with Substituted Acrylonitriles[a]

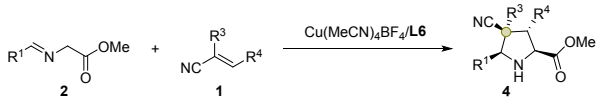

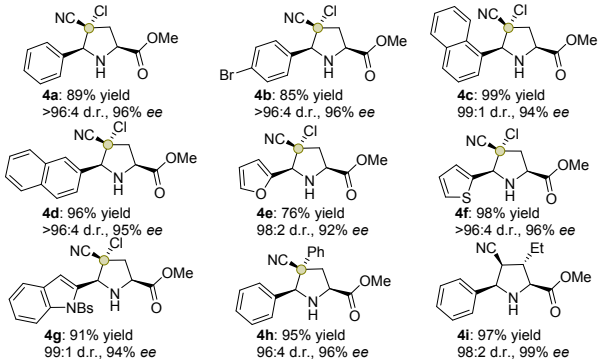

[a]Conditions unless otherwise stated: **1** (0.4 mmol), **2** (0.2 mmol), **L6** (5.5 mol%), $Cu(MeCN)_4BF_4$ (5 mol%), Et_3N (50 mol%), 4 Å MS (200 mg), CH_2Cl_2 (4 mL), 0 °C or room temperature, 16–48 h; the d.r. is the ratio of endo/exo isomers, determined by HPLC or ^1H NMR analysis of the crude reaction mixture; the *ee* was determined by chiral HPLC analysis of the endo isomer; **4i** was prepared under the conditions given in Table 2.

Table 4. Catalytic Asymmetric 1,3-Dipolar Cycloaddition of Various Iminoesters with Unsubstituted Acrylonitrile[a]

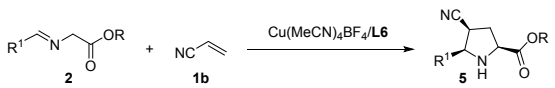

entry	5	R¹/R	yield (%)[b]	d.r.[c]	*ee* (%)[d]
1	**5a**	Ph/Me	95	99:1	99
2	**5b**	4-F-C_6H_4/Me	90	99:1	99
3	**5c**	4-Cl-C_6H_4/Me	85	99:1	99
4	**5d**	4-Br-C_6H_4/Me	86	99:1	99
5	**5e**	4-Me-C_6H_4/Me	82	96:4	99
6	**5f**	4-MeO-C_6H_4/Me	87	99:1	99
7	**5g**	4-Me_2N-C_6H_4/Me	77	99:1	98
8	**5h**	4-CN-C_6H_4/Me	90	98:2	98
9	**5i**	4-COOMe-C_6H_4/Me	87	98:2	98
10	**5j**	4-CF_3-C_6H_4/Me	95	98:2	99
11	**5k**	4-NO_2-C_6H_4/Me	82	99:1	98
12	**5l**	2-Br-C_6H_4/Me	88	99:1	99
13	**5m**	3-Br-C_6H_4/Me	84	97:3	99
14	**5n**	2-F-C_6H_4/Me	89	99:1	97
15	**5o**	3-F-C_6H_4/Me	97	95:5	97
16	**5p**	1-naphthyl/Me	82	98:2	99
17	**5q**	2-naphthyl/Me	86	97:3	99
18	**5r**	2-thienyl/Me	87	97:3	99
19	**5s**	2-furyl/Me	86	96:4	97
20	**5t**	*N*-Bn-2-pyrryl/Me	75	97:3	97
21	**5u**	3-pyridyl/Me	87	99:1	98
22	**5v**	*N*-Bs-2-indolyl/Me	80	98:2	95
23	**5w**	Ph/Et	98	98:2	98
24	**5x**	Ph/^{i}Pr	91	99:1	98
25	**5y**	Ph/^{t}Bu	91	99:1	98
26	**5z**	Ph/Bn	90	98:2	99

[a]Conditions: **1b** (0.4 mmol), **2** (0.2 mmol), **L6** (5.5 mol%), $Cu(MeCN)_4BF_4$ (5 mol%), Et_3N (50 mol%), 4 Å MS (200 mg), CH_2Cl_2 (4 mL), 0 °C, 16–48 h. [b]Yield of the isolated endo isomer. [c]Ratio of the endo/exo isomers, determined by HPLC analysis of the crude reaction mixture. [d]Determined by chiral HPLC analysis of the endo isomer.

We also expanded this methodology to 1,3-dipolar cycloaddition of unsubstituted acrylonitrile (Table 4). In theory, 1,3-dipolar cycloaddition of unsubstituted acrylonitrile should be less challenging than methacrylonitrile, because it is more reactive and good stereocontrol is easier to access in the absence of an α methyl group. Indeed, there are a few highly enantioselective catalytic systems that tolerate unsubstituted acrylonitrile as the dipolarophile.[8] However, a systematic investigation of the scope of iminoesters has not been reported. A wide range of iminoester **2** were examined using the bifunctional catalyst. Iminoesters with electron-deficient groups or electron-rich groups on the phenyl ring gave the cycloaddition products in good yields (77–95%) with excellent stereoselectivities (98:2–99:1 d.r., 98–99% *ee*) (entries 1–11). The substitution pattern on the phenyl ring has no obvious effect on the reactivity and stereoselectivity, and *ortho*-, *meta*-, and *para*-substituted substrates are all tolerated in this cycloaddition (entries 2, 4, and 12–15). Fused aromatic 1- and 2-naphthyl-substituted glycine imines are also suitable azomethine ylide precursors (entries 16 and 17). Remarkably, iminoesters substituted with a variety of heteroaryl groups, including thienyl, pyrryl, pyridyl, and indolyl groups, all worked well in this transformation (entries 18–22). When iminoesters with different ester groups are used, excellent yields and stereoselectivities are achieved (entries 23–26).

The substrate scope was further expanded to include *α*-substituted iminoesters (Scheme 2). We did not observe any obvious difference between iminoesters derived from L- and D-amino acid esters in terms of the reaction rate, yield, or stereoselectivity (**6a–6c**). Remarkably, the catalytic system could tolerate the co-presence of *α*-substituents on the iminoester and acrylonitrile, providing direct access to chiral pyrrolidine **6d** with two quaternary stereogenic centers,

therefore, highlighting the generality of this 1,3-dipolar cycloaddition protocol.

Scheme 2. Catalytic Asymmetric 1,3-Dipolar Cycloaddition of α-Substituted Iminoesters

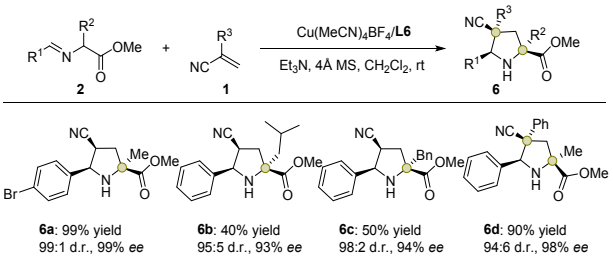

The relative and absolute configurations for all of the five different types of cycloaddition products were determined by single-crystal X-ray crystallographic analysis (Figure 8, **3d**, ***N*-(*P*-Br)Bz-4a**, **5d**, ***N*-Ts-6a**, and **6d**),[18,28] and the same configuration were analogously assigned to the other products.

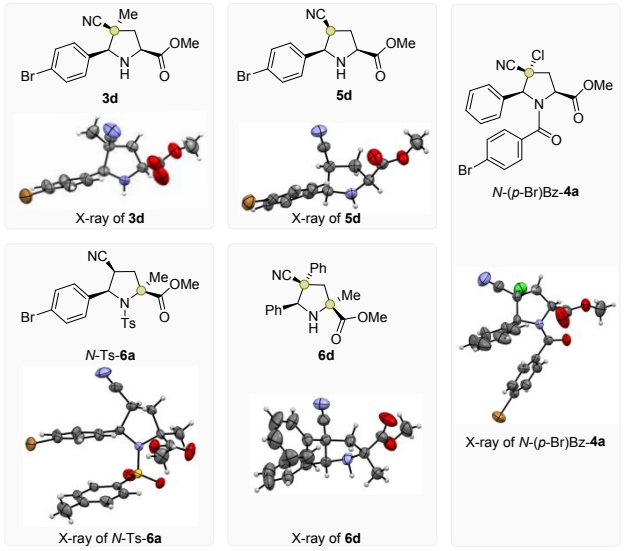

Figure 8. X-ray structures of the representative cycloadducts.

Synthetic Applications. The synthetic utility of this protocol was further investigated (Scheme 3). The reaction between **2p** and **1a** was performed on the gram-scale to test the scalability of this cycloaddition reaction. Compound **3p** was obtained in 65% yield with 95:5 d.r. and 97% *ee*. According to Overman's report on preparation of (±)-**ETP69**,[9b] reaction of

Scheme 3. Gram-Scale 1,3-Dipolar Cycloaddition and Enantioselective Synthesis of ETP69

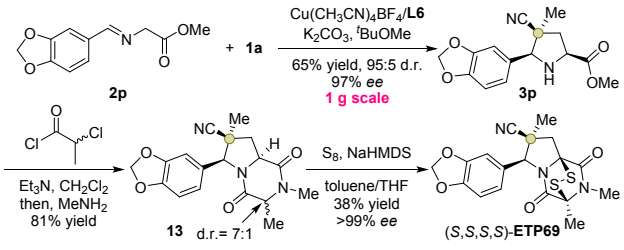

enantioenriched product **3p** with 2-chloropropinyl chloride and then with $MeNH_2$ results in formation of dioxopiperazine **13**, which transforms to **ETP69** in 38% yield by treatment with NaHMDS/S_8. Using our 1,3-dipolar cycloaddition protocol and the following two-step reaction sequence, almost enantiopure (>99% *ee*) (*S*,*S*,*S*,*S*)-**ETP69** was conveniently synthesized.

■ CONCLUSIONS

We have developed a novel simple type of chiral amidophosphine–urea bifunctional ligands. By combining metal-catalysis and organocatalysis, the first catalytic enantioselective 1,3-dipolar cycloaddition of iminoesters with methacrylonitrile has been realized in high yields with excellent diastereo- and enantioslectivities (up to 99:1 d.r., 99% *ee*). A wide substrate scope of both iminoesters and acrylonitriles can be tolerated by the catalyst system of **L6**/Cu, producing a series of chiral pyrrolidine derivatives with up to two quaternary stereogenic centers. Using this protocol, enantioselective synthesis of the nitrile pharmacophore-bearing antitumor agent **ETP69** has been successfully achieved. DFT with the M11 functional was used to investigate the origin of the enantio- and diastereoselectivity of asymmetric 1,3-dipolar cycloaddition. The DFT calculations indicate that nucleophilic addition is the enantioselectivity-determining step and the hydrogen bonding between the urea moiety and methacrylonitrile assists in controlling the diastereo- and enantioselectivity. Distortion–interaction energy analysis based on DFT calculations reveals that the distortion energy plays an important role in the observed enantioselectivity, which can be attributed to the steric effect between the phosphine ligand and the dipole reactant. Furthermore, *N*-methylated phosphine–urea ligands were designed, synthesized, and tested for asymmetric 1,3-dipolar cycloaddition, demonstrating that hydrogen bonding (organocatalysis) is crucial for the high reactivity and stereoselectivity. This combined theoretical and experimental study shows that synergistic activation and spatial orientation of the dipole and dipolarophile by effective integration of metal-catalysis and organocatalysis are responsible for the high reaction efficiency and excellent stereoselectivity for 1,3-dipolar cycloaddition of iminoesters with acrylonitriles.

ASSOCIATED CONTENT

Supporting Information

The Supporting Information is available free of charge on the ACS Publications website.

Experimental procedures and compound characterization (PDF)

Crystallographic structure of **3d** (CIF)

Crystallographic structure of *N*-(*P*-Br)Bz-**4a** (CIF)

Crystallographic structure of **5d** (CIF)

Crystallographic structure of *N*-Ts-**6a** (CIF)

Crystallographic structure of **6d** (CIF)

AUTHOR INFORMATION

Corresponding Author

*Email: minzhang@cqu.edu.cn

*Email: lanyu@cqu.edu.cn

Author Contributions

§These authors contributed equally to this work.

ACKNOWLEDGMENT

This work was supported by NSFC (21402015, 21672029, 21772020, 21822303) and Chongqing Provincial Human Resources and Social Security Department (CX2017048). We are grateful to Prof. Weiping Tang and Ms. Stephanie A. Blaszczyk (UW-Madison) for helpful discussions and proofreading the manuscript, and Mr. Xiangnan Gong (CQU) for X-ray crystallographic analysis.

REFERENCES

(1) Walsh, P. J.; Kozlowski, M. C. *Fundamentals of Asymmetric Catalysis*; University Science Books: Sausalito, CA, **2009**.

(2) (a) Fadini, L.; Togni, A. Nickel(II) Complexes Containing Chiral Tridentate Phosphines as New Catalysts for the Hydroamination of Activated Olefins. *Chem. Commun.* **2003**, 30. (b) Sadow, A. D.; Togni, A. Enantioselective Addition of Secondary Phosphines to Methacrylonitrile: Catalysis and Mechanism. *J. Am. Chem. Soc.* **2005**, *127*, 17012. (c) Chen, Y.; Ruppel, J. V.; Zhang, X. P. Cobalt-Catalyzed Asymmetric Cyclopropanation of Electron-Deficient Olefins. *J. Am. Chem. Soc.* **2007**, *129*, 12074. (d) Carmona, D.; Lamata, M. P.; Viguri, F.; Rodríguez, R.; Lahoz, F. J.; Fabra, M. J.; Oro, L. A. Asymmetric 1,3-Dipolar Cycloaddition Reaction of α,β-Unsaturated Nitriles with Nitrones Catalyzed by Chiral-at-Metal Rhodium or Iridium Complexes. *Tetrahedron: Asymmetry* **2009**, *20*, 1197. (e) Carmona, D.; Viguri, F.; Asenjo, A.; Lamata, P.; Lahoz, F. J.; García-Orduña, P. Asymmetric 1,3-Dipolar Cycloaddition Reactions Between Methacrylonitrile and Nitrones Catalyzed by Well-Defined M(diphosphine) (M = Rh, Ir) Complexes. *Tetrahedron: Asymmetry* **2016**, *27*, 454.

(3) For selected reviews, see: (a) Gothelf, K. V.; Jørgensen, K. A. Asymmetric 1,3-Dipolar Cycloaddition Reactions. *Chem. Rev.* **1998**, *98*, 863. (b) Coldham, I.; Hufton, R. Intramolecular Dipolar Cycloaddition Reactions of Azomethine Ylides. *Chem. Rev.* **2005**, *105*, 2765. (c) Nájera, C.; Sansano, J. M. Catalytic Enantioselective 1,3-Dipolar Cycloaddition Reaction of Azomethine Ylides and Alkenes: the Direct Strategy to Prepare Enantioenriched Highly Substituted Proline Derivatives. *Angew. Chem. Int. Ed.* **2005**, *44*, 6272. (d) Pandey, G.; Banerjee, P.; Gadre, S. R. Construction of Enantiopure Pyrrolidine Ring System via Asymmetric [3+2]-Cycloaddition of Azomethine Ylides. *Chem. Rev.* **2006**, *106*, 4484. (e) Naodovic, M.; Yamamoto, H. Asymmetric Silver-Catalyzed Reactions. *Chem. Rev.* **2008**, *108*, 3132. (f) Stanley, L. M.; Sibi, M. P. Enantioselective Copper-Catalyzed 1,3-Dipolar Cycloadditions. *Chem. Rev.* **2008**, *108*, 2887. (g) Adrio, J.; Carretero, J. C. Novel Dipolarophiles and Dipoles in the Metal-Catalyzed Enantioselective 1,3-Dipolar Cycloaddition of Azomethine Ylides. *Chem. Commun.* **2011**, *47*, 6784. (h) Adrio, J.; Carretero, J. C. Recent Advances in the Catalytic Asymmetric 1,3-Dipolar Cycloaddition of Azomethine Ylides. *Chem. Commun.* **2014**, *50*, 12434. (i) Narayan, R.; Potowski, M.; Jia, Z. J.; Antonchick, A. P.; Wadmann, H. Catalytic Enantioselective 1,3-Dipolar Cycloadditions of Azomethine Ylides for Biology-Oriented Synthesis. *Acc. Chem. Res.* **2014**, *47*, 1296. (j) Hashimoto, T.; Maruoka, K. Recent Advances of Catalytic Asymmetric 1,3-Dipolar Cycloadditions. *Chem. Rev.* **2015**, *115*, 5366.

(4) For the pioneering works of catalytic asymmetric 1,3-dipolar cycloadditions of iminoesters, see: (a) Longmire, J. M.; Wang, B.; Zhang, X.–M. Highly Enantioselective Ag(I)-Catalyzed [3 + 2] Cycloaddition of Azomethine Ylides. *J. Am. Chem. Soc.* **2002**, *124*, 13400. (b) Gothelf, A. S.; Gothelf, K. V.; Hazell, R. G.; Jørgensen, K. A. Catalytic Asymmetric 1,3-Dipolar Cycloaddition Reactions of Azomethine Ylides-A Simple Approach to Optically Active, Highly Functionalized Proline Derivatives. *Angew. Chem. Int. Ed.* **2002**, *41*, 4236.

(5) For selected examples of metal-involved 1,3-dipolar cycloadditions of iminoesters, see: (a) Chen, C.; Li, X.; Schreiber, S. L. Catalytic Asymmetric [3+2] Cycloaddition of Azomethine Ylides. Development of a Versatile Stepwise, Three-Component Reaction for Diversity-Oriented Synthesis. *J. Am. Chem. Soc.* **2003**, *125*, 10174. (b) Yan, X.-X; Peng, Q.; Zhang, Y.; Zhang, K.; Hong, W.; Hou, X.-L.; Wu, Y.-D. A Highly Enantioselective and Diastereoselective Cu-Catalyzed 1,3-Dipolar Cycloaddition of Azomethine Ylides with Nitroalkenes. *Angew. Chem. Int. Ed.* **2006**, 45, 1979. (c) Saito, S.; Tsubogo, T.; Kobayashi, S. Chiral Calcium Complexes as Bronsted Base Catalysts for Asymmetric Addition of α-Amino Acid Derivatives to α,β-Unsaturated Carbonyl Compounds. *J. Am. Chem. Soc.* **2007**, *129*, 5364. (d) López-Pérez, A.; Adrio, J.; Carretero, J. C. Bis-Sulfonyl Ethylene as Masked Acetylene Equivalent in Catalytic Asymmetric [3 + 2] Cycloaddition of Azomethine Ylides. *J. Am. Chem. Soc.* **2008**, *130*, 10084. (e) Nájera, C.; Retamosa, M. de G.; Sansano. J. M. Catalytic Enantioselective 1,3-Dipolar Cycloaddition Reactions of Azomethine Ylides and Alkenes by Using Phosphoramidite-Silver(I) Complexes. *Angew. Chem. Int. Ed.* **2008**, *47*, 6055. (f) Wang, C.-J.; Liang, G.; Xue, Z.-Y.; Gao. F. Highly Enantioselective 1,3-Dipolar Cycloaddition of Azomethine Ylides Catalyzed by Copper(I)/TF-BiphamPhos Complexes. *J. Am. Chem. Soc.* **2008**, *130*, 17250. (g) López-Pérez, A.; Adrio, J.; Carretero, J. C. The Phenylsulfonyl Group as A Temporal Regiochemical Controller in the Catalytic Asymmetric 1,3-Dipolar Cycloaddition of Azomethine Ylides. *Angew. Chem. Int. Ed.* **2009**, *48*, 340. (h) Arai, T.; Mishiro, A.; Yokoyama, N.; Suzuki, K.; Sato, H. Chiral Bis(imidazolidine)pyridine-Cu(OTf)2: Catalytic Asymmetric Endo-Selective [3 + 2] Cycloaddition of Imino Esters with Nitroalkenes. *J. Am. Chem. Soc.* **2010**, *132*, 5338. (i) Arai, T.; Yokoyama, N.; Mishiro, A.; Sato, H. Catalytic Asymmetric exo'-Selective [3+2] Cycloaddition of Iminoesters with Nitroalkenes. *Angew. Chem. Int. Ed.* **2010**, *49*, 7895. (j) Zhang, C.; Yu, S.-B.; Hu, X.-P.; Wang, D.-Y.; Zheng, Z.-O. New Chiral Ferrocenyl P,S-Ligands for Highly Diastereo-/Enantioselective Catalytic [3 + 2] Cycloaddition of Azomethine Ylides with Cyclic and Acyclic Enones. *Org. Lett.* **2010**, *12*, 5542. (k) Kim, H. Y.; Li, J. Y.; Kim, S.; Oh, K. Stereodivergency in Catalytic Asymmetric Conjugate Addition Reactions of Glycine (Ket)imines. *J. Am. Chem. Soc.* **2011**, *133*, 20750. (l) Wang, M.; Wang, Z.; Shi, Y.-H.; Shi, X.-X.; Fossey, J. S.; Deng, W. P. An exo- and Enantioselective 1,3-Dipolar Cycloaddition of Azomethine Ylides with Alkylidene Malonates Catalyzed by a N,O-Ligand/Cu(OAc)2-Derived Chiral Complex. *Angew. Chem. Int. Ed.* **2011**, *50*, 4897. (m) Hernández-Toribio, J.; Padilla, S.; Adrio, J.; Carretero, J. C. Catalytic Asymmetric Synthesis of α-Quaternary Proline Derivatives by 1,3-Dipolar Cycloaddition of α-Silylimines. *Angew. Chem. Int. Ed.* **2012**, *51*, 8854. (n) Potowski, M.; Bauer, J. O.; Strohmann, C.; Antonchick, A. P.; Waldmann, H. Highly Enantioselective Catalytic [6+3] Cycloadditions of Azomethine Ylides. *Angew. Chem. Int. Ed.* **2012**, *51*, 9512. (o) He, Z.-L.; Teng, H.-L.; Wang, C.-J. Fulvenes as Effective Dipolarophiles in Copper(I)-Catalyzed [6+3] Cycloaddition of Azomethine Ylides: Asymmetric Construction of Piperidine Derivatives. *Angew. Chem. Int. Ed.* **2013**, *52*, 2934. (p) Narayan, R.; Bauer, J. O.; Strohmann, C.; Antonchick, A. P.; Waldmann, H. Catalytic Enantioselective Synthesis of Functionalized Tropanes Reveals Novel Inhibitors of Hedgehog Signaling. *Angew. Chem. Int. Ed.* **2013**, *52*, 12892. (q) Awata, A.; Arai, T. PyBidine/Copper catalyst. Asymmetric exo'-Selective [3+2] Cycloaddition Using Imino Ester and Electrophilic Indole. *Angew. Chem. Int. Ed.* **2014**, *53*, 10462. (r) Li, Q.-H.; Wei, L.; Wang, C.-J. Catalytic Asymmetric 1,3-Dipolar [3 + 6] Cycloaddition of Azomethine Ylides with 2-Acyl Cycloheptatrienes: Efficient Construction of Bridged

Heterocycles Bearing Piperidine Moiety. *J. Am. Chem. Soc.* **2014**, *136*, 8685. (s) Liu, H.; Wu, Y.; Zhao, Y.; Li, Z.; Zhang, L.; Yang, W.; Jiang, H.; Jing, C.; Yu, H.; Wang, B.; Xiao, Y.; Guo, H. Metal-Catalyzed [6 + 3] Cycloaddition of Tropone with Azomethine Ylides: A Practical Access to Piperidine-Fused Bicyclic Heterocycles. *J. Am. Chem. Soc.* **2014**, *136*, 2625. (t) Teng, H.-L.; Yao, L.; Wang, C.-J. Cu(I)-Catalyzed Regio- and Stereoselective [6 + 3] Cycloaddition of Azomethine Ylides with Tropone: An Efficient Asymmetric Access to Bridged Azabicyclo[4.3.1]Decadienes. *J. Am. Chem. Soc.* **2014**, *136*, 4075. (u) Bai, X.-F.; Song, T.; Xu, Z.; Xia, C.-G.; Huang, W.-S.; Xu, L.-W. Aromatic Amide-Derived Non-Biaryl Atropisomers as Highly Efficient Ligands in Silver-Catalyzed Asymmetric Cycloaddition Reactions. *Angew. Chem. Int. Ed.* **2015**, *54*, 5255. (v) Pascual-Escudero, A.; de Cózar, A.; Cossío, F. P.; Adrio, J.; Carretero, J. C. Alkenyl Arenes as Dipolarophiles in Catalytic Asymmetric 1,3-Dipolar Cycloaddition Reactions of Azomethine Ylides. *Angew. Chem. Int. Ed.* **2016**, *55*, 15334. (w) Zhang, Z.-M.; Xu, B.; Xu, S.; Wu, H.-H.; Zhang, J.-L. Diastereo- and Enantioselective Copper(I)-Catalyzed Intermolecular [3+2] Cycloaddition of Azomethine Ylides with β-Trifluoromethyl β,β-Disubstituted Enones. *Angew. Chem. Int. Ed.* **2016**, *55*, 6324. (x) Xu, Y.; Liao, Y.; Lin, L.; Zhou, Y.; Li, J. Liu, X.; Feng, X. Catalytic Asymmetric Inverse-Electron Demand 1,3-Dipolar Cycloaddition of Isoquinolinium Methylides with Enecarbamates by a Chiral *N,N'*-Dioxide/Ag(I) Complex. *Acs Catal.* **2016**, *6*, 589. (y) Xu, S.; Zhang, Z.-M.; Xu, B.; Liu, B.; Liu, Y.; Zhang, J.-L. Enantioselective Regiodivergent Synthesis of Chiral Pyrrolidines with Two Quaternary Stereocenters via Ligand-Controlled Copper(I)-Catalyzed Asymmetric 1,3-Dipolar Cycloadditions. *J. Am. Chem. Soc.* **2018**, *140*, 2272. (z) Feng, B.; Lu, L.-Q.; Chen, J.-R.; Feng, G.; He, B.-Q.; Lu, B.; Xiao, W.-J. Umpolung of Imines Enables Catalytic Asymmetric Regio-reversed [3+2] Cycloadditions of Iminoesters with Nitroolefins. *Angew. Chem. Int. Ed.* **2018**, *57*, 5888.

(6) For selected examples of organocatalytic 1,3-dipolar cycloadditions of iminoesters, see: (a) Chen, X.-H.; Zhang, W.-Q.; Gong, L.-Z. Asymmetric Organocatalytic Three-Component 1,3-Dipolar Cycloaddition: Control of Stereochemistry via a Chiral Bronsted Acid Activated Dipole. *J. Am. Chem. Soc.* **2008**, *130*, 5652. (b) Liu, Y.-K.; Liu, H.; Du, W.; Yue, L.; Chen, Y.-C. Reaction Control in the Organocatalytic Asymmetric One-Pot, Three-Component Reaction of Aldehydes, Diethyl α-Aminomalonate and Nitroalkenes: toward Diversity-Oriented Synthesis. *Chem. Eur. J.* **2008**, *14*, 9873. (c) Chen, X.-H.; Wei, Q.; Luo, S.-W.; Xiao, H.; Gong, L.-Z. Organocatalytic Synthesis of Spiro[pyrrolidin-3,3'-oxindoles] with High Enantiopurity and Structural Diversity. *J. Am. Chem. Soc.* **2009**, *131*, 13819. (d) He, L.; Chen, X.-H.; Wang, D.-N.; Luo, S.-W.; Zhang, W.-Q.; Yu, J.; Ren, L.; Gong, L.-Z. Binaphthol-Derived Bisphosphoric Acids Serve as Efficient Organocatalysts for Highly Enantioselective 1,3-Dipolar Cycloaddition of Azomethine Ylides to Electron-Deficient Olefins. *J. Am. Chem. Soc.* **2011**, *133*, 13504. (e) Lin, S.-Z.; Deiana, L.; Zhao, G.-L.; Sun, J.-L.; Córdova, A. Dynamic One-Pot Three-Component Catalytic Asymmetric Transformation by Combination of Hydrogen-Bond-Donating and Amine Catalysts. *Angew. Chem. Int. Ed.* **2011**, *50*, 7624.

(7) For selected examples that H-bonding was proposed to be involved in the metal-involved 1,3-dipolar cycloadditions, see: (a) Zeng, W.; Chen, G.-Y.; Zhou, Y.-G.; Li, Y.-X. Hydrogen-Bonding Directed Reversal of Enantioselectivity. *J. Am. Chem. Soc.* **2007**, *129*, 750. (b) Kim, H. Y.; Shih, H. J.; Knabe, W. E.; Oh, K. Reversal of Enantioselectivity between the Copper(I)- and Silver(I)-Catalyzed 1,3-Dipolar Cycloaddition Reactions Using a Brucine-Derived Amino Alcohol Ligand. *Angew. Chem. Int. Ed.* **2009**, *48*, 7420. (c) Liu, T.-L.; He, Z.-L.; Tao, H.-Y.; Wang, C.-J. Stereoselective Construction of Spiro(butyrolactonepyrrolidines) by Highly Efficient Copper(I)/TF-BiphamPhos-Catalyzed Asymmetric 1,3-Dipolar Cycloaddition. *Chem. Eur. J.* **2012**, *18*, 8042. (d) Wang, M.; Wang, C.-J.; Lin, Z. Cu(I)/TF-BiphamPhos Catalyzed Reactions of Alkylidene Bisphosphates and Alkylidene Malonates with Azomethine Ylides: Michael Addition versus 1,3-Dipolar Cycloaddition. *Organometallics* **2012**, *31*, 7870. (e) Arai, T.; Ogawa, H.; Awata, A.; Sato, M.; Watabe, M.; Yamanaka, M. PyBidine-Cu(OTf)2-Catalyzed Asymmetric [3+2] Cycloaddition with Imino Esters: Harmony of Cu-Lewis Acid and Imidazolidine-NH Hydrogen Bonding in Concerto Catalysis. *Angew. Chem. Int. Ed.* **2015**, *54*, 1595.

(8) For dipolarophiles containing a nitrile group, see: (a) Cabrera, S.; Arrayás, R. G.; Carretero, J. C. Highly Enantioselective Copper(I)-Fesulphos-Catalyzed 1,3-Dipolar Cycloaddition of Azomethine Ylides. *J. Am. Chem. Soc.* **2005**, *127*, 16394. (b) Nájera, C.; de Gracia Retamosa, M.; Sansano, J. M.; de Cózar, A.; Cossío, F. P. Enantioselective Synthesis of Polysubstituted Prolines by Binap-Silver-Catalyzed 1,3-Dipolar Cycloadditions. *Tetrahedron: Asymmetry* **2008**, *19*, 2913. (c) Eröksüz, S.; Dogan, Ö.; Garner, P. P. A New Chiral Phosphine Oxide Ligand for Enantioselective 1,3-Dipolar Cycloaddition Reactions of Azomethine Ylides. *Tetrahedron: Asymmetry* **2010**, *21*, 2535. (d) Padilla, S.; Tejero, R.; Adrio, J.; Carretero, J. C. N-(2-Pyridylmethyl)Imines as Azomethine Precursors in Catalytic Asymmetric [3 + 2] Cycloadditions. *Org. Lett.* **2010**, *12*, 5608. (e) Yamashita, Y.; Imaizumi, T.; Guo, X.-X.; Kobayashi, S. Chiral Silver Amides as Effective Catalysts for Enantioselective [3+2] Cycloaddition Reactions. *Chem. Asian J.* **2011**, *6*, 2550. (f) Yamashita, Y.; Imaizumi, T.; Kobayashi, S. Chiral Silver Amide Catalyst for the [3+2] Cycloaddition of α-Amino Esters to Olefins. *Angew. Chem. Int. Ed.* **2011**, *50*, 4893. (g) Maroto, E. E.; Filippone, S.; Martin-Domenech, A.; Suarez, M.; Martin, N. Switching the Stereoselectivity: (Fullero)Pyrrolidines "a la Carte". *J. Am. Chem. Soc.* **2012**, *134*, 12936. (h) Chaulagain, M. R.; Felten, A. E.; Gilbert, K.; Aron, Z. D. Diastereo- and Enantioselective Three-Component Coupling Approach to Highly Substituted Pyrrolidines. *J. Org. Chem.* **2013**, *78*, 9471. (i) Joseph, R.; Murray, C.; Garner, P. Catalytic Asymmetric exo-Selective [C+NC+CC] Reaction. *Org. Lett.* **2014**, *16*, 1550.

(9) (a) Walton, M. C.; Yang, Y.-F.; Hong, X.; Houk, K. N.; Overman, L. E. Ligand-Controlled Diastereoselective 1,3-Dipolar Cycloadditions of Azomethine Ylides with Methacrylonitrile. *Org. Lett.* **2015**, *17*, 6166. (b) Baumann, M.; Dieskau, A. P.; Loertscher, B. M.; Walton, M. C.; Nam, S.; Xie, J.; Horne, D.; Overman, L. E. Tricyclic Analogues of Epidithiodioxopiperazine Alkaloids with Promising in Vitro and in Vivo Antitumor Activity. *Chem. Sci.* **2015**, *6*, 4451. Soon afterwards, the Overman group demonstrated that **ETP69** also improves cognition in aged hippocampus by inhibition of H3K9mes, see: (c) Snigdha, S.; Prieto, G. A.; Petrosyan, A.; Loertscher, B. M.; Dieskau, A. P.; Overman. L. E.; Cotman, C. W. H3K9me3 Inhibition Improves Memory, Promotes Spine Formation, and Increases BDNF Levels in the Aged Hippocampus. *J. Neurosci.* **2016**, *36*, 3611.

(10) Zhang, Q.-Z.; Zhang, Z.-S.; Huang, Z.; Zhang, C.-H; Xi, S.; Zhang, M. Stereoselective Total Synthesis of Hetisine-Type C20-Diterpenoid Alkaloids: Spirasine IV and XI. *Angew. Chem. Int. Ed.* **2018**, *57*, 937.

(11) For selected reviews, see: (a) Shibasaki, M.; Yoshikawa, N. Lanthanide Complexes in Multifunctional Asymmetric Catalysis. *Chem. Rev.* **2002**, *102*, 2187. (b) Ma, J.-A.; Cahard, D. Towards Perfect Catalytic Asymmetric Synthesis: Dual Activation of the Electrophile and the Nucleophile. *Angew. Chem. Int. Ed.* **2004**, *43*, 4566. (c) Shao, Z.-H.; Zhang, H.-B. Combining Transition Metal Catalysis and Organocatalysis: A Broad New Concept for Catalysis. *Chem. Soc. Rev.* **2009**, *38*, 2745. (d) Meeuwissen, J.; Reek, J. N. H. Supramolecular Catalysis Beyond Enzyme Mimics. *Nature Chem.* **2010**, *2*, 615. (e) Zhong, C.; Shi, X.-D. When Organocatalysis Meets Transition-Metal Catalysis. *Eur. J. Org. Chem.* **2010**, 2999; (f) Zhou, J. Recent Advances in Multicatalyst

Promoted Asymmetric Tandem Reactions. *Chem. Asian J.* **2010**, *5*, 422. (g) Du, Z.-T.; Shao, Z.-H. Combining Transition Metal Catalysis and Organocatalysis-an Update. *Chem. Soc. Rev.* **2013**, *42*, 1337. (g) Zhou, J. *Multicatalyst System in Asymmetric Catalysis*; John Wiley & Sons: New York, **2014**.

(12) For selected examples, see: (a) Xu, Z.-H.; Liu, L.; Wheeler, K.; Wang, H. Asymmetric Inverse-Electron-Demand Hetero-Diels-Alder Reaction of Six-membered Cyclic Ketones: An Enamine/Metal Lewis Acid Bifunctional Approach. *Angew. Chem. Int. Ed.* **2011**, *50*, 3484. (b) Sladojevich, F.; Trabocchi, A.; Guarna, A.; Dixon, D. J. A New Family of Cinchona-Derived Amino Phosphine Precatalysts: Application to the Highly Enantio- and Diastereoselective Silver-Catalyzed Isocyanoacetate Aldol Reaction. *J. Am. Chem. Soc.* **2011**, *133*, 1710. (c) Zhao, Q.-Y.; Li, S.-K.; Huang, K.-X.; Wang, R.; Zhang, X.-M. A Novel Chiral Bisphosphine-Thiourea Ligand for Asymmetric Hydrogenation of β,β-Disubstituted Nitroalkenes. *Org. Lett.* **2013**, *15*, 4014. (d) Zhao, Q.-Y.; Wen, J.-L.; Tan, R.-C.; Huang, K.-X.; Metola, P.; Wang, R.; Anslyn, E. V.; Zhang, X.-M. Rhodium-Catalyzed Asymmetric Hydrogenation of Unprotected NH Imines Assisted by a Thiourea. *Angew. Chem. Int. Ed.* **2014**, 53, 8467. (e) Yuan, Z.-B.; Wei, W.-W.; Lin, A.-J.; Yao, H.-Q. Bifunctional Organo/Metal Cooperatively Catalyzed [3 + 2] Annulation of para-Quinone Methides with Vinylcyclopropanes: Approach to Spiro[4.5]deca-6,9-diene-8-ones. *Org. Lett.* **2016**, *18*, 3370.

(13) Part of this work was applied for a China patent by us, see: Zhang, M.; Xiong, Y.; Du, Z.-Z; Tang, P. CN 107383095A, 20171124.

(14) For a recent review on ligands with a phosphinoamide unit, see: Štěpnička, P. Phosphino-carboxamides. The Inconspicuous Gems. *Chem. Soc. Rev.* **2012**, *41*, 4273.

(15) For selected reviews, see: (a) Taylor, M. S.; Jacobsen, E. N. *Angew.* Asymmetric Catalysis by Chiral Hydrogen-Bond Donors. *Chem. Int. Ed.* **2006**, *45*, 1520. (b) Ian Storer, R.; Aciro, C.; Jones, L. H. Squaramides: Physical Properties, Synthesis and Applications. *Chem. Soc. Rev.* **2011**, *40*, 2330.

(16) For selected reviews on synthesis of quaternary stereogenic centers, see: (a) Quasdorf, K. W.; Overman, L. E. Catalytic Enantioselective Synthesis of Quaternary Carbon Stereocentres. *Nature*, **2014**, *516*, 181. (b) Büschleb, M.; Dorich, S.; Hanessian, S.; Tao, D.; Schenthal, K. B.; Overman, L. E. Synthetic Strategies toward Natural Products Containing Contiguous Stereogenic Quaternary Carbon Atoms. *Angew. Chem. Int. Ed.* **2016**, 55, 4156.

(17) For a selected review on chiral sulfur ligands, see: Mellah, M.; Voituriez, A.; Schulz, E. Chiral Sulfur Ligands for Asymmetric Catalysis. *Chem. Rev.* **2007**, *107*, 5133.

(18) See the Supporting Information for details.

(19) Frisch, M. J. Gaussian 09, Revision D.01; Gaussian, Inc., Wallingford, CT, **2013**. The full author list is shown in the Supporting Information.

(20) Peverati, R.; Truhlar, D. G. Improving the Accuracy of Hybrid Meta-GGA Density Functionals by Range Separation. *J. Phys. Chem. Lett.* **2011**, *2*, 2810.

(21) (a) Dolg, M.; Stoll, H.; Preuss, H. Energy-adjusted ab initio pseudo potentials for the rare earth elements. *J. Chem. Phys.* **1989**, *90*, 1730. (b) Dolg, M.; Wedig, U.; Stoll, H.; Preuss, H. Energy-Adjusted Ab Initio Pseudo Potentials for the First Row Transition Elements. *J. Chem. Phys.* **1987,** *86*, 866. (c) Liu, S.; Qi, X.; Qu, L.-B.; Bai, R.; Lan, Y. C–H Bond Cleavage Occurring on a Rh(v) Intermediate: a Theoretical Study of Rh-Catalyzed Arene Azidation. *Catal. Sci. Technol.* **2018**, *8*, 1645. (d) Qi, X.; Li, Y.; Bai, R.; Lan, Y. Mechanism of Rhodium-Catalyzed C-H Functionalization: Advances in Theoretical Investigation. *Acc. Chem. Res.* **2017**, *50*, 2799. (e) Lu, G.; Liu, R. Y.; Yang, Y.; Fang, C.; Lambrecht, D. S.; Buchwald, S. L.; Liu, P. Ligand–Substrate Dispersion Facilitates the Copper-Catalyzed Hydroamination of Unactivated Olefins. *J. Am. Chem. Soc.* **2017**, *139*, 16548. (f) Qi, X.; Liu, X.; Qu, L.-B.; Liu, Q.; Lan, Y. Mechanistic Insight into Cobalt-Catalyzed Stereodivergent Semihydrogenation of Alkynes: The Story of Selectivity Control. *J. Catal.* **2018,** *362*, 25.

(22) (a) Peverati, R.; Truhlar, D. G. Improving the Accuracy of Hybrid Meta-GGA Density Functionals by Range Separation. *J. Phys. Chem. Lett.* **2011**, *2*, 2810. (b) Shan, C.; Zhu, L.; Qu, L.-B.; Bai, R.; Lan, Y. Mechanistic View of Ru-Catalyzed C-H Bond Activation and Functionalization: Computational Advances. *Chem. Soc. Rev.* **2018**, *47*, 7552.

(23) (a) Cossi, M.; Barone, V.; Cammi, R.; Tomasi. J. Ab Initio Study of Solvated Molecules: a New ImplemEntation of the Polarizable Continuum Model. *Phys. Chem. Lett.* **1996**, *255*, 327. (b) Cances, E.; Mennunci, B.; Tomasi, J. A New Integral Equation Formalism for the Polarizable Continuum Model: Theoretical Background and Applications to Isotropic and Anisotropic Dielectrics. *J. Chem. Phys.* **1997**, *107*, 3032. (c) Barone, V.; Cossi, M.; Tomasi, J. Geometry Optimization of Molecular Structures in Solution by the Polarizable Continuum Model. *J. Comput. Chem.* **1998**, *19*, 404. (d) Mekareeya, A.; Walker, P. R.; Couce-Rios, A.; Campbell, C. D.; Steven, A.; Paton, R. S.; Anderson, E. A. Mechanistic Insight into Palladium-Catalyzed Cycloisomierzation: A Combined Experimental and Theoretical Study. *J. Am. Chem. Soc.* **2017**, *139*, 10104. (e) Shi, H.; Michaelides, L. N.; Darses, B.; Jakubec, P.; Nguyen, Q. N. N.; Paton, R. S.; Dixon, D. J. Total Synthesis of (-)-Himalensine A. *J. Am. Chem. Soc.* **2017**, *139*, 17755.

(24) (a) Liu, S.; Lei, Y.; Qi, X.; Lan, Y. Reactivity for the Diels-Alder Reaction of Cumulenes: A Distortion-Interaction Analysis along the Reaction Pathway. *J. Phys. Chem. A.* **2014**, *118*, 2638. (b) Jin, R.; Liu, S.; Lan, Y. Distortion-Interaction Analysis Along the Reaction Pathway to Reveal the Reactivity of the Alder-Ene Reaction of Enes. *RSC Adv.* **2015**, 5, 61426. (c) Huang, J.; Gu, Y.; Guo, K.; Zhu, L.; Lan, Y.; Gong, J.; Yang, Z. Bioinspired Total Synthesis of Homodimericin A. *Angew. Chem. Int. Ed.* **2017**, *56*, 7890. (d) Ni, H.; Yu, Z.; Yao, W.; Lan, Y.; Ullah, N.; Lu, Y. Catalyst-Controlled Regioselectivity in Phosphine Catalysis: The Synthesis of Spirocyclic Benzofuranones via Regiodivergent [3 + 2] Annulations of Aurones and an Allenoate. *Chem. Sci.* **2017**, *8*, 5699. (e) Burrows, L. C.; Jesikiewicz, L. T.; Lu, G.; Geib, S. J.; Liu, P.; Brummond, K. M. *J. Am. Chem. Soc.* **2017**, *139*, 15022. (f) Cui, C.-X.; Shan, C.; Zhang, Y.-P.; Chen, X.-L.; Qu, L.-B.; Lan, Y. Mechanism of Phosphine-Catalyzed Allene Coupling Reactions: Advances in Theoretical Investigations. *Chem. Asian J.* **2018**, *13*, 1076.

(25) For a recent review on halogenated natural products, see: Wang, B. G.; Gloer, J. B.; Ji, N. Y.; Zhao, J. C. Halogenated Organic Molecules of Rhodomelaceae Origin: Chemistry and Biology. *Chem. Rev.* **2013**, *113*, 3632–3685.

(26) For selected reviews on the halogenation, see: (a) Denmark, S. E.; Kuester, W. E.; Burk, M. T. Catalytic, Asymmetric Halofunctionalization of Alkenes. A Critical Perspective. *Angew. Chem. Int. Ed.* **2012**, *51*, 10938. (b) Cresswell, A. J.; Eey, S. T.-C.; Denmark, S. E. Catalytic, Stereoselective Dihalogenation of Alkenes: Challenges and Opportunities. *Angew. Chem. Int. Ed.* **2015**, *54*, 15642. (c) Chung, W.-j.; Vanderwal, C. D. Stereoselective Halogenation in Natural Product Synthesis. *Angew. Chem. Int. Ed.* **2016**, 55, 4396.

(27) Tan, Q.-Y.; Wang, X.-Q.; Xiong, Y.; Zhao, Z.-M.; Li, L.; Tang, P.; Zhang, M. Chiral Amino Alcohol Accelerated and Stereocontrolled Allylboration of Iminoisatins: Highly Efficient Construction of Adjacent Quaternary Stereogenic Centers. *Angew. Chem. Int. Ed.* **2017**, *56*, 4829.

(28) CCDC 1818884 (**3d**), CCDC 1575775 (**5d**), CCDC 1575127 (**6d**), and CCDC 1575128 (*N*-(*p*-Br)Bz-**4a**), and CCDC 1575112 (*N*-Ts-**6a**) contain the supplementary crystallographic data for this paper. These data can be obtained free of charge from The Cambridge Crystallographic Data Centre. Note: for **6d** with no heavy atom incorporated, only relative configurations were determined.

Table of Contents artwork: